

Air Force Institute of Technology

AFIT Scholar

Faculty Publications

2016

Short-term Building Energy Model Recommendation System: A Meta-learning Approach

Can Cui

Arizona State University

Teresa Wu

Arizona State University

Mengqi Hu

The University of Illinois at Chicago

Jefferey D. Weir

Air Force Institute of Technology

Xiwang Li

Arizona State University

Follow this and additional works at: <https://scholar.afit.edu/facpub>



Part of the [Systems Engineering Commons](#)

Recommended Citation

Cui, C., Wu, T., Hu, M., Weir, J. D., & Li, X. (2016). Short-term building energy model recommendation system: A meta-learning approach. *Applied Energy*, 172(15 June), 251–263. <https://doi.org/10.1016/j.apenergy.2016.03.112>

This Article is brought to you for free and open access by AFIT Scholar. It has been accepted for inclusion in Faculty Publications by an authorized administrator of AFIT Scholar. For more information, please contact richard.mansfield@afit.edu.

Short-Term Building Energy Model Recommendation System: A Meta-Learning Approach

Can Cui^a

School of computing, informatics, and decision systems engineering
Arizona State University
699 S. Mill Ave., Tempe, AZ 85281, USA
ccan1@asu.edu

Teresa Wu^a (Corresponding author)

Room 308, 699 S. Mill Ave., Tempe, AZ 85281, USA
Teresa.Wu@asu.edu, 1-(480)-965-4157

Mengqi Hu^b

Department of Mechanical and Industrial Engineering
University of Illinois at Chicago
842 W. Taylor St., Chicago, IL 60607
mhu@uic.edu

Jeffery D. Weir^c

Department of operational sciences
Air Force Institute of Technology
2950 Hobson Way, Wright-Patterson Afb, Ohio 45433, USA
Jeffery.Weir@afit.edu

Xiwang Li^d

Center for Green Buildings and Cities, Graduate School of Design
Harvard University
20 Sumner Rd, Cambridge, MA, 02138
xiwang_li@gsd.harvard.edu

Abstract

High-fidelity and computationally efficient energy forecasting models for building systems are needed to ensure optimal automatic operation, reduce energy consumption, and improve the building's resilience capability to power disturbances. Various models have been developed to forecast building energy consumption. However, given buildings have different characteristics and operating conditions, model performance varies. Existing research has mainly taken a trial-and-error approach by developing multiple models and identifying the best performer for a specific building, or presumed one universal model form which is applied on different building cases. To the best of our knowledge, there does not exist a generalized system framework which can recommend appropriate models to forecast the building energy profiles based on building characteristics. To bridge this research gap, we propose a meta-learning based framework, termed Building Energy Model Recommendation System (BEMR). Based on the building's physical features as well as statistical and time series meta-features extracted from the operational data and energy consumption data, BEMR is able to identify the most appropriate load forecasting model for each unique building. Three sets of experiments on 48 test buildings and one real building are conducted. The first experiment is to test the accuracy of BEMR when the training data and testing data cover the same condition. BEMR correctly identified the best model on 90% of the buildings. The second experiment is to test the robustness of the BEMR when the testing data is only partially covered by the training data. BEMR correctly identified the best model on 83% of the buildings. The third experiment uses a real building case to validate the proposed framework and the result shows promising applicability and extensibility. The experimental results show that BEMR is capable of adapting to a wide variety of

49 building types ranging from a service restaurant to a large office, and gives excellent performance in terms
50 of both modeling accuracy and computational efficiency.
51

52 **Keywords**

53 Building energy consumption; time series forecasting; recommendation system; machine learning; meta-
54 learning; feature reduction;
55

56 **1 INTRODUCTION**

57 According to the U.S. Energy Information Administration (EIA), buildings consume nearly half (48%)
58 of the total energy and produce almost 45% of CO₂ emissions in the United States [1]. This drives the need
59 to develop high-fidelity and computationally efficient energy forecasting models for building systems to
60 ensure optimal automatic operation, reduce energy consumption, and improve the building's resilience
61 capability to power grid disturbances [2]. Existing building energy models are in general categorized as:
62 physics-based models, hybrid models and data-driven models (Li and Wen 2014). Physics-based
63 models employ the physical concepts and knowledge of the low level devices and aggregate the
64 mathematical expressions to model the building system. It heavily relies on domain expertise and often is
65 computationally prohibitive [4]. Hybrid models use simplified physical descriptions combined with
66 parameter identification algorithms to predict energy consumption. Nevertheless, without a description of
67 the building geometry and materials, it is difficult to estimate the model parameters. In contrast, the
68 emerging technology advancements in the energy industry make it possible to collect massive amounts of
69 data from sensors and meters, which enable data-driven modeling to unfold the underlying knowledge [5].
70 As most industrial, institutional, and commercial buildings built after 2000 include a building automation
71 systems (BAS), there is a growing interest to mine valuable information and derive additional insights
72 from data collected. The data-driven approach motivates and drives the building energy research in various
73 aspects including estimation of energy consumption [6]–[8], real-time performance validation and energy
74 usage analysis [9], and energy saving operational control [3], [10], [11]. A significant advantage of the data
75 driven approach lies in that it considerably reduces the design cycle iteration time for building design and
76 operations, which includes not only simulation, but also analysis of results and optimization of actions
77 based on these results. It allows for fast realizations of the design and operation tasks for any building
78 scenario in an industrial context. Based on the updating cycle and horizon, the load forecast models can
79 also be categorized into short term load forecasting (STLF), medium term load forecasting (MTLF), and
80 long term load forecasting (LTLF) [12]. STLF focuses on the load forecasting on daily basis and/or
81 weekly basis, and MTLF and LTLF are based on monthly and yearly collected data for transmission and
82 distribution (T&D) planning [13], and financial planning, which assist with medium to long term energy
83 management, decision making on the utilities project and revenue management. STLF is important for
84 real-time energy operations and maintenance. For daily operations, system operators can make switching
85 and operational decisions, and schedule maintenance based on the patterns obtained during the load
86 forecasting process [14]. To better assist the operations and control strategies development, this study
87 develops a novel STLF methodology for buildings, which provides accurate load forecasts for daily and
88 weekly based energy system management. The model, however, could be viably transformed into MTLF
89 or LTLF, by adding features of economy and land use, and extrapolating the model to longer horizons.

90 Various data-driven methods have been studied and implemented for building load forecasting
91 including 1) statistical methods such as autoregressive, moving average, exponential smoothing [15], state
92 space [16], [17], polynomial regression [18], and 2) machine learning methods such as neural
93 networks [19] and support vector regression [8], [20]. Statistical regression models simply build the
94 correlation between the energy consumption and the simplified influential features such as weather
95 parameters. These empirical models are developed from historical performance data to train the models.

96 Machine learning models are good at building non-linear models and are especially effective on complex
97 applications.

98 A regression-based approach was tested on the peak and hourly load forecasts of the next 24 hours
99 using Pacific Gas and Electric Company's (PG&E) data [21]. The regression model was thoroughly tested
100 and concluded to be superior to the existing system load forecasting algorithms used at PG&E. In another
101 study, five methods (autoregressive integrated moving average (ARIMA) modeling; periodic AR modeling,
102 an extension for double seasonality of Holt-Winters exponential smoothing; an alternative
103 exponential smoothing formulation; and a principle component analysis (PCA) based method) were
104 compared on 10 load series from 10 European countries on an hourly interval and 24-hour horizon [22].
105 They concluded that the double seasonal Holt-Winters exponential smoothing method outperformed the
106 others. Another interesting study by Ahmed, Atiya, Gayar, & El-Shishiny (2010) explored machine
107 learning methods. Eight machine learning models for time series forecasting on the monthly M3 time series
108 competition data (around a thousand time series) were investigated. These eight are multilayer perceptron,
109 Bayesian neural networks, radial basis functions, generalized regression neural networks, K-nearest
110 neighbor regression, CART regression trees, support vector regression, and Gaussian processes. They
111 concluded that the best two methods turned out to be the multilayer perceptron and the Gaussian process
112 regression. Chirattananon and Taveekun (2004) developed a model for building energy consumption
113 forecasting based on overall thermal transfer value and concluded that the model does not present good
114 generalizability on some types of buildings, especially on hotels and hospitals. Yik, Burnett, and Prescott
115 (2001) predicted the energy consumption for a group of different types of buildings using a number of
116 physical parameters such as air conditioning system type, year the building was built and geographical
117 information. The resulting model showed high correlation to the detailed simulation model. One novel
118 data-characteristic-driven modeling methodology for nuclear energy consumption was proposed in [26],
119 in which two steps, data analysis and forecasting modeling, were involved in formulating an appropriate
120 forecasting model in terms of the sample data's own data characteristics. Experimental results showed
121 that "data-characteristic-driven modeling" significantly improves prediction performance compared to all
122 other benchmark models without consideration of data characteristics. However, only time series data
123 characteristics and univariate forecasting models were explored in this study. One observation from these
124 extensive studies is model performance varies and is highly dependent on the characteristics of the
125 building systems, which leads the researchers to come to inconsistent conclusions regarding the performance
126 of various forecasting models. This concurs with what was found by [27]: he thoroughly reviewed
127 twenty-five years of research and concluded that no algorithm is best for all load forecasting tasks. He
128 suggested that the identification of which methods should be chosen with respect to the situations should
129 be done via experimental studies.

130 Noting that a building system is stochastic, nonlinear and complex [28], research so far has mainly
131 focused on an approach of trial-and-error or one-size-fits-all. In the cases where little prior knowledge of
132 the building systems is available, previous studies either develop multiple models and identify the
133 outperformer among them, which is computationally expensive and impractical for real-time building
134 energy management and operations, or subjectively presume one model fits any type of building, suffering
135 from high-bias modeling. In short-term building load forecasting, the main goal is to minimize the
136 forecasting error with computationally-efficient solutions. Building management control tasks can range
137 from real-time load forecasting and user behavior analysis to predictive building control. For these tasks,
138 the meter data are usually generated at a rate ranging from per minute to per hour. Due to the dynamics of
139 building energy systems and for real-time supervisory purposes, the control and operations should be
140 updated dynamically by analyzing the time series data. This impedes the trial-and-error modeling
141 approach in that the computational complexity for constructing multiple models is unaffordable,
142 especially in the case where data volume is large. In a broader scope, a reduction of the forecasting error
143 ensures the power systems stabilize in balance and assists power market design, operation, and security of
144 supply [29]. These drive the need for a general framework for short-term building load forecasting, which
145 satisfies both the time constraint driven by real-time building operations and control, and the fidelity

146 constraint which calls for high-accuracy load forecasting. The general building load forecasting
147 framework would be beneficial in dealing with heterogeneous building load forecasting tasks for most
148 commercial utilities and market participants. Taking into account the above, we develop a Building
149 Energy Model Recommendation (BEMR) system for short-term load forecasting motivated by the meta-
150 learning concept. Meta-learning has gained increasing attention and has been successfully applied in
151 diverse research fields including gene expression classification [30], failure prediction [31], gold market
152 forecasting (Zhou, Lai, & Yen, 2012), and electric load forecasting [33], just to name a few. Meta-learning
153 is a machine learning algorithm that explores the learning process and understands the mechanism of the
154 process, which can be re-used for future learning. The objective is to build a self-adaptive automatic
155 learning mechanism that connects the meta-data (e.g., the characteristics of the problems) with the model
156 performance. As a result, the best performing model can be identified via the meta-data directly and thus
157 significantly saving the model training process.

158 Earlier efforts on meta-learning for forecasting mainly focused on rule-based approaches. For
159 example, [34] weighted four candidate models using 99 derived rules from human experts' analysis. The
160 weight of each model is modified based on the features of the time series. One potential issue of this
161 approach is the knowledge acquired from human experts may not be easily accessible. Prudêncio &
162 Ludermir (2004) used a decision tree on a stationary time series with two candidate
163 algorithms, exponential smoothing with a neural network, and NOEMON, on the M3-competition time
164 series, for ranking three candidate models: random walk, Holt's smoothing, and auto-regressive. They
165 concluded both case studies revealed satisfactory results, taking into account the quality in the selection
166 and the forecasting performance of the selected models. Wang, Smith-Miles, & Hyndman (2009)
167 generated a decision tree on the induced rules from univariate time series data characteristics, where four
168 algorithms: Random walk, smoothing, ARIMA, and neural network, were selected as candidates. They
169 were able to draw recommendations and suggestions on the conceptive, categorical and quantitative
170 rules. The meta-learning system based on a large pool of meta-features proposed by [37] was shown to
171 outperform many approaches of the NN3 and NN5 competition entries. Marin Matijaš, Suykens, &
172 Krajcar (2013) proposed a meta-learning system for load forecasting based on multivariate time series, in
173 which 65 load forecasting tasks in Europe were tested and lower forecasting errors were observed
174 compared to 10 well-known forecasting algorithms.

175 Note that the literature reviewed above all attempt to gain knowledge from time series data to
176 generate rules which define the relationship between the meta-features and the model performance. While
177 promising for the problems examined, building systems are inherently nonlinear, diverse and complex
178 due to the heterogeneity among multiple interconnected factors, e.g., internal factors, social factors and
179 weather factors [28]. For buildings, especially large and complex ones, simplifications of model
180 formulations and lack of physical knowledge may lead to poor forecast accuracy. Therefore, the meta-
181 knowledge characterization should not solely be collected from the building's operational data, such as
182 energy consumption univariate time series, but also the building's physical features.

183 We conclude that a generalized intelligent system for building energy model recommendation, which
184 incorporates both building data-characteristic and physical-characteristic meta-features is currently
185 lacking and this research attempts to fill this gap motivated by the research success from [39]. Specifically,
186 we employ a two-stage meta-learning approach for BEMR. It first trains multiple models on the existing
187 buildings to obtain the model performance. Next, the features and/or meta-features are derived from the
188 existing building instances in association with the respective performances for making recommendations
189 on the new building. The BEMR framework developed in this study can be used on development and
190 selection of models for building energy modeling and forecasting, as well as building optimal operation
191 and real-time control.

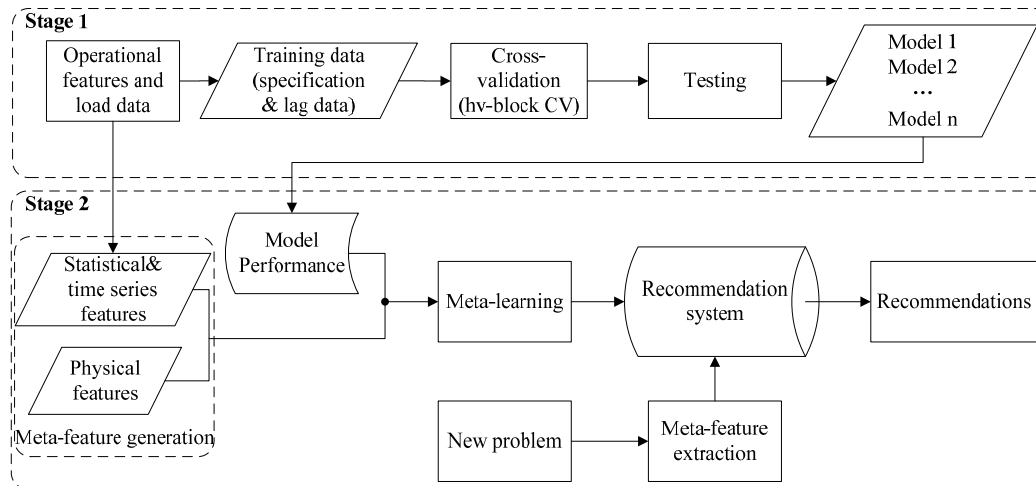
192 In developing BEMR, the first notable challenge is that building data is of high dimension in both the
193 temporal and spatial domains. Building energy consumption is influenced by many factors: internal
194 factors such as building structure and physical characteristics, the sub-system components like equipment
195 schedule and operations on HVAC systems, occupants and their behavior, and external factors such as

196 natural environments, weather conditions, and economies. Therefore, meta-features are introduced to
197 depict the operational data, and the physical features of the buildings are gathered as additional
198 descriptive knowledge. We hypothesize the inclusion of the heterogeneous features should increase the
199 generalization of BEMR for diverse buildings in different operating conditions. Next, six statistical and
200 machine learning data-driven models are explored and included in BEMR: Kriging, support vector
201 regression (SVR), radial basis function (RBF), multivariate adaptive regression splines (MARS), artificial
202 neural network (ANN) and polynomial regression (PR). These models are chosen due to their extensive
203 use in surrogate modeling applications [40] and their good theoretical and experimental performance on
204 energy system applications [41], [42]. The third effort in BEMR is to collect the building instances as the
205 training sources. Considering that both the building type (internal factors) and climates (external factors)
206 have effects on energy consumption profiles, 48 (8 building types on 6 climate zones) simulated
207 commercial and residential reference buildings developed by the Department of Energy (DOE) are
208 collected. Last, ANN is chosen as the meta-learner to develop the associations between the meta-features
209 derived from the building instances and the model performance so the best model is identified. Three sets
210 of experiments are conducted using leave-one-out cross validation. The first experiment is to test the
211 performance of BEMR on regular short-term daily and weekly forecasting. Experiment results show that
212 among the 48 buildings, BEMR is able to identify the best model for 43 buildings (accuracy: 90%) and
213 the difference of the mean of the normalized root mean square error (NRMSE) from the ground truth is
214 within 2%. The second experiment is to validate the robustness of BEMR when the test data is only
215 partially covered by the training data, and we call it extrapolation validation. Among the 48 buildings, 40
216 (accuracy: 83%) correct model recommendations are made and the difference of mean NRMSE from the
217 ground truth is within 3%. Moreover, the computational cost of the system is significantly lower than
218 traditional trial-and-error approaches, which decreases forecast time from the order of minutes to
219 seconds. The third experiment is to validate the proposed framework on a real building case, which is
220 located in Ankeny, IA. The result shows that the proposed BEMR is capable of making reliable
221 recommendations for a real building energy forecast.

222 The paper is constructed as follows: Section 2 introduces the proposed methodology; Experiments and
223 results are discussed in Section 3; finally, a discussion of the conclusion and future work is given in
224 Section 4. The appendix gives a brief discussion on the data-driven forecasting algorithms.
225

226 **2 BUILDING ENERGY MODEL RECOMMENDATION SYSTEM**

227 In this research, we propose a Building Energy Model Recommendation System (BEMR) for short-
228 term building energy consumption forecasting. BEMR is a two-stage framework. As shown in Figure
229 1, the first stage is to establish the instance repository to connect the learning instances with a forecasting
230 models' performance; next, both building physical features and operational meta-features are derived and
231 connected with the model performances so the model recommendation can be made.
232



233
234
235

Figure 1 Framework of Building Energy Model Recommendation (BEMR) System

236 2.1 Stage I: Building Learning Instance Repository

237 Eight types of commercial and residential buildings are selected from the DOE simulated reference
 238 buildings which are identified as the most prevalent building types [43] in the United States. Considering
 239 the significant impact of climate on the energy consumption profile, each building type is simulated
 240 at each of six selected locations which correspond to the climate zones discussed in ASHRAE 90.1 -
 241 2004 [44]. These locations are San Francisco, CA; Boulder, NV; Phoenix, AZ; Houston, TX; Miami, FL;
 242 and Baltimore, MD. As a result, the building repository includes a total of 48 simulated buildings (8 types,
 243 in 6 locations). The corresponding TMY3 (typical meteorological year) weather data sets [45] are adopted
 244 as the weather data source for the simulation models.

245 2.1.1 Training Data Selection

246 The STLF process heavily relies on the weather information and ambient environment. When the
 247 parameters are estimated, the weather information is extrapolated to forecast the load. Much research [4],
 248 [20] has looked at the most suitable features for load forecast problems. They try to explain the causality
 249 of the electric load consumption. In STLF, the electric load is generally driven by nature and human
 250 activities. Nature is usually represented by weather variables, e.g., temperature and humidity, while the
 251 human activities are usually represented by the calendar variables, e.g., occupancy and business hours.
 252 High-dimensional feature spaces result in unnecessary complication in building forecasting models and
 253 thus impede the optimization process. To alleviate this concern, our features are selected based on the
 254 work of Eisenhower et al. (2012), in which the sensitivity analyses were conducted to identify the most
 255 influential features for the energy output generated from the EnergyPlus simulation models. They were
 256 adopted to develop the meta-model and the following optimization model for energy management
 257 operations. Seventy influential variables, which are all temperature and human activity related, were
 258 selected to build a reduced form of meta-models. On the foundation of their work, 12 operational features
 259 are initially selected from over 600 features in the simulation models, including (1) outdoor air dry bulb
 260 temperature; (2) outdoor air relative humidity; (3) outdoor air flow rate; (4) diffuse solar radiation rate; (5)
 261 direct solar radiation rate; (6) zone people occupant count; (7) zone air temperature; (8) zone air relative
 262 humidity; (9) zone thermostat cooling set point temperature; (10) building equipment schedule; (11)
 263 building light schedule; (12) HVAC operation schedule. In addition, since periodicity is one main
 264 characteristic in electricity load time series, two categorical variables, Day and Time are added to the
 265 study. Given these 14 features, we then conduct principal component analysis (PCA) [46] to explore the

266 multicollinearity among the features for robust forecasting model development. It is observed that feature
 267 11 (building light schedule) and feature 12 (HVAC operation schedule) are highly correlated with feature
 268 9 (zone thermostat cooling set point temperature). Therefore, these two highly collinear variables are
 269 removed from the study. We further assess the correlation between each remaining feature and the
 270 response variable using Pearson’s correlation coefficient. It is observed that all the features are
 271 significantly correlated to the response variable (the absolute correlations are all above the threshold
 272 correlation, 0.195, to reject the null hypothesis that the two variables are not correlated). Note categorical
 273 variables are excluded in the multicollinearity test and the correlation test. Finally, ten building operational
 274 features and two categorical variables are selected (Table 1).
 275

276 Table 1. Ten Selected Building Operational Features and two Categorical Variables

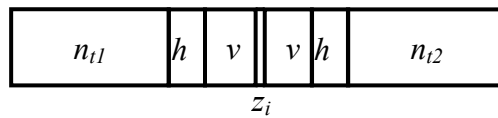
	Building Variables	Variable Type [range]
1	Outdoor Air Drybulb Temperature (°C)	Continuous
2	Outdoor Air Relative Humidity	Continuous on [0,1]
3	Outdoor Air Flow Rate	Continuous
4	Diffuse Solar Radiation Rate (W/m ²)	Continuous
5	Direct Solar Radiation Rate (W/m ²)	Continuous
6	Zone People Occupant Count	Integer
7	Zone Air Temperature (°C)	Continuous
8	Zone Air Relative Humidity	Continuous on [0,1]
9	Zone Thermostat Cooling SetPoint Temperature (°C)	Continuous
10	Building Equipment Schedule Value	Continuous on [0,1]
11	Day of Week	Integer on [1,7]
12	Time of Day	Integer on [1,48]

277 Besides the features discussed above, all the buildings (simulation models) apply typical equipment
 278 control strategies for chillers and fans. In fact, no matter how the subsystems/devices are controlled, their
 279 operations will be reflected in the training data. Our models should be able to capture these operation
 280 characteristics in the model training process. The objective of this study is to provide whole building level
 281 STLF models for building operation and control. As a result, only the building level features are selected.
 282 The detailed sub-system level and device level operation are not studied in this paper.
 283

284 For the features, both specification data and lagged data are collected in the training data set.
 285 Specifically, let c be the periodicity of the seasonality, n be the number of lags, and t be the current time
 286 data index, then the specification data indices are $t, t - c, t - 2c$, while the lagged data indices are $t-1, t -$
 287 $2, \dots, t-n$. For example, assume the current time t is 12 pm on a day, possible lagged data indices are
 288 11:30 pm, 11 pm, 10:30 pm, etc. (given data are collected every 30 minutes), and possible specification
 289 data indices are 12 pm in the past few days ($c=24$ hrs.). This is motivated by the “Similar Days technique”
 290 in [47] that a particular load on the same day of the week should behave similarly, given similar weather
 291 and other conditions. Several researchers have pointed out the superior performance of specification
 292 models over traditional models which are built solely on lagged data (Crespo Cuaresma, Hlouskova,
 293 Kossmeier, & Obersteiner, 2004).
 294

295 **2.1.2 Cross validation**

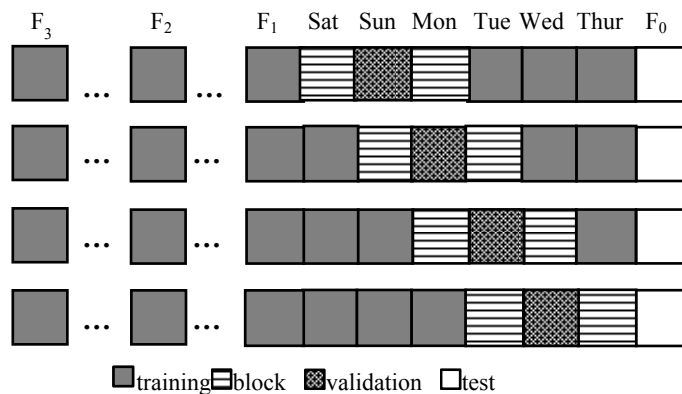
296 It is worth noting that in traditional forecasting, a common practice is to reserve some data toward the
 297 end of each time series for testing, and to use earlier time series data for training. One potential issue is
 298 that the data are not fully made use of due to a lack of cross-validation, and the resulting model may suffer
 299 from over-fitting. Meanwhile, for time series data it may not be appropriate to directly apply traditional
 300 cross-validation, which randomly splits the data into training and testing datasets. Theoretical problems
 301 with respect to temporal evolutionary effects and data dependencies are encountered when the fundamental
 302 assumptions of cross-validation might be invalidated. Racine (2000) proposes “ $h\nu$ -block” cross-validation
 303 which is asymptotically optimal. It is consistent for temporally dependent observations in the sense that
 304 the probability of selecting the model with the best predictive ability converges to 1 as the total number of
 305 observations approaches infinity. The basic idea is to place restrictions on the relationship between
 306 the training set, validation set, the size of an h -block, and the sample size. We can thereby obtain a
 307 consistent cross-validating model selection procedure for the process.
 308



309
 310 Figure 2 “ $h\nu$ -block” Cross-validation Illustration

311 As shown in Figure 2, given an observation z_i , we first remove ν observations on either side of it to
 312 obtain a validation set of size $2\nu+1$. We then remove another h observations on either side of this validation
 313 set with the remaining $n-2\nu-2h-1$ observations forming the training set. The value of ν controls the size of
 314 the validation set with $n_\nu = 2\nu+1$. The value of h controls the dependence of the training set of size $n_t = n -$
 315 $2h - n_\nu$ and the validation set of size n_ν . For guidance on appropriate selection on h and ν , please refer to
 316 [48] for details.

317 For illustration, Figure 3 shows the design for cross-validation on a single day test. Take Friday as an
 318 example, and let’s define it as F_0 , and the unit of lag being a day, with n being 6 days, and c being 7 days.
 319 Therefore, the training data consists of six days of lagged data (Thursday, Wednesday, Tuesday, Monday,
 320 and Sunday on the same week of test data, and Saturday from the previous week) and three days of
 321 specification data (three Fridays from the last three weeks, F_1, F_2, F_3). Based on the “ $h\nu$ -block” cross-
 322 validation approach, the training data are cross split into 4 training and validation folds. In each fold, the
 323 size of validation data n_ν and the block h are set as one day, and the rest of data is kept aside as training
 324 data.



325
 326 Figure 3 Cross-validation of Training Data Split

2.1.3 Forecasting Model Performance Evaluation

In BEMR, six data-driven models are explored including Kriging, support vector regression (SVR), radial basis function (RBF), multivariate adaptive regression splines (MARS), artificial neural network (ANN) and polynomial regression (PR). To make the recommendation, the first step is to evaluate and validate the model performance using available building energy data. The performance is measured using Normalized Root Mean Square Error (NRMSE), where

$$NRMSE = \sqrt{\frac{\sum_{i=1}^N (y_i - \hat{y}_i)^2}{N}} / (y_{max} - y_{min}), \quad (1)$$

and y is the true value of the building energy consumption and \hat{y} is the forecast value.

In summary, stage I of the BEMR is providing the base repository which consists of 288 models (8 building types, 6 locations, 6 data driven models) and the respective forecasting performance (measured by NRMSE). This enables the implementation of the meta-learning strategy which is discussed in the next section.

2.2 Stage II: Meta-level Learning

2.2.1 Meta-Feature Extraction

Meta-features, which characterize the entire dataset for meta-level induction learning, are an abstraction of knowledge extracted from the dataset. Three types of meta-features are devised, including physical features, statistical features and time series features. Table 2 summarizes the seven physical features of the buildings.

Table 2 Building Physical Features

Feature #	1	2	3	4	5	6	7
Building Type	# of stories	Area(m ²)	Roof Type	Wall Type	Window Type	Cooling	Space Type
Large Office	12 ¹	46,320	IEAD ²	Mass	Fixed	Chiller, water-cooled	Non-residential
Medium Office	3	4,982	IEAD ²	Steel Frame	Fixed	Packaged DX ³	Non-residential
Small Office	1	511	Attic Roof	Mass	Fixed	Packaged DX ³	Non-residential
Supermarket	1	4,181	IEAD ²	Mass	Fixed	Packaged DX ³	Non-residential
Full Service Restaurant	1	511	Attic Roof	Steel Frame	Fixed	Packaged DX ³	Non-residential
Hospital	5 ¹	22,422	IEAD ²	Mass	Fixed	Chiller, water-cooled	Residential for patient rooms
Large Hotel	6 ¹	11,345	IEAD ²	Mass	Operable in guest rooms	Chiller, air-cooled	Residential for guest rooms
Midrise Apartment	4	3,135	IEAD ²	Steel Frame	Operable	Packaged DX ³	Residential

¹ Plus Basement.

² Built-up flat roof with insulation entirely above the roof deck.

³ Packaged Direct-expansion (DX) equipment.

Other than the seven physical meta-features, nine statistical meta-features similar to (Matijaš, 2013; Lemke & Gabrys, 2010) are derived from the operational features from Table 1 and the energy consumption data:

(S1) Min: e.g., the minimum of load over a time period

- 356 (S2) Max: e.g., the maximum of load over a time period
 357 (S3) Mean: e.g., arithmetic average of load over a time period
 358 (S4) SD: e.g., the standard deviation of load over a time period
 359 (S5) Skewness: evaluates the lack of symmetry, taking the load as an example, Y_i is the load of timeperiod
 360 i , and \bar{Y} is the mean of the load over a period of time, skewness is derived as:

$$361 \quad E \{[(Y_i - \bar{Y})/Std. (Y_i)]^3\}, i = 1, \dots, N, \quad (2)$$

- 362 (S6) Kurtosis: evaluates the flatness relative to a normal distribution. Again, taking the load as an
 363 example

$$364 \quad E [(Y_i - \bar{Y})^4] / (E[(Y_i - \bar{Y})^2])^2, i = 1, \dots, N, \quad (3)$$

- 365 (S7) Q1: e.g., 25% quartile of load, which is the lower quartile of load.
 366 (S8) Q2: e.g., 50% quartile of load, which is the median of load.
 367 (S9) Q3: e.g., 75% quartile of load, which is the upper quartile of load.

368
 369 In addition, considering the building system is dynamic and non-linear, we introduce four time series
 370 meta-features to describe the temporal characteristics of the building energy data.

- 371
 372 (T1) Ratio of local extrema: Ratio of local minima and maxima within a given neighborhood, taking the
 373 load as an example, it measures the percentage of load oscillation.
 374 (T2) Non-linearity: A number of surrogate data is generated from the null hypothesis that the series is
 375 linear, and the derived estimate of the original time series data is compared to the ones generated
 376 from the surrogate data to check the non-linearity [49].
 377 (T3) Cut-off lag of ACF: The autocorrelation function (ACF) is the collection of the autocorrelation
 378 coefficients, which indicate the covariance between observations with any lag. In this study, a lag of
 379 30 autocorrelation coefficients is calculated.
 380 (T4) Cut-off lag of PACF: Similarly, a lag 30 of the partial autocorrelation function (PACF) is used to
 381 derive the coefficients.

382
 383 As a result, we derive nine statistical meta-features for each of the ten building operational data and
 384 the energy consumption data (99 meta-features in total). Additionally, four time series meta-features on
 385 the energy consumption data are derived. With the seven building physical features a total of 110 features
 386 (meta-features) are used for meta-learning.
 387

388 2.2.2 Meta-learner

389 [50], [51] indicate that a powerful artificial intelligence-based model is more preferable than
 390 traditional statistical models. Therefore, we use an ANN as the meta-learner, considering correlation
 391 between the meta-features and nonlinear patterns brought by the complexity and heterogeneities of
 392 different building scenarios (noises within meta-features) might impair the modeling power of the learner.
 393 The parameter settings of the meta-learner ANN areas follows: the hidden layer size is tuned within the
 394 range of [10, 20], and the transfer functions are selected between radial basis and log sigmoid. Note that
 395 the proposed meta-features are tentatively selected in hoping that they could effectively represent the
 396 dataset. However, the number of features is more than twice the number of problems, which may impair
 397 the predictive power of the meta-learner. This is known as the “Hughes effects” [52]. As a result, we
 398 propose to use an advanced feature reduction technique to address the curse of dimensionality.
 399 Specifically, singular value decomposition (SVD) is of interest in this research due to its known
 400 performance on noise filtering and dimensionality reduction. It is a factorization of a real matrix $X \in R^{m \times n}$,
 401 $m \geq n$,

$$402 \quad X = USV^t, \quad (4)$$

403 where $U \in R^{m \times m}$ and $V \in R^{n \times n}$ are orthogonal matrices and $S \in R^{m \times n}$ is a diagonal matrix. A rank- k
 404 ($k \ll \min(m, n)$) matrix C is defined as the best low-rank approximation of matrix X if it minimizes the
 405 Frobenius norm of the matrix $(X - C)$, which is known as the Eckart–Young theorem [53]. This
 406 approximation matrix can be computed by SVD factorization and keeping the first k columns of U ,
 407 truncating S to the first k diagonal components, and keeping the first k rows of V^t . This results in noise
 408 reduction by assuming the matrix X is low rank, which is not generated at random but has an underlying
 409 structure.
 410

411 2.2.3 BEMR Performance Evaluation

412 Given the predicted rankings of the six models’ performance from the recommendation system, two
 413 evaluation metrics are introduced to evaluate the meta-learning performance: The Spearman’s rank
 414 correlation coefficient (SRCC) and success rate.

415 The Spearman’s rank correlation coefficient [54] is employed to measure the agreement between
 416 recommended rankings and ideal rankings on a forecasting problem. For two samples of size N , the rank
 417 coefficient is computed as

$$418 \rho = 1 - 6 \cdot \frac{\sum_{i=1}^N d_i^2}{N(N^2-1)} \quad (5)$$

419 where $d_i = r_i - l_i$, and r_i and l_i are the recommended rank and the ideal rank on the i^{th} sample. In this case,
 420 the sample size N is the number of candidate forecasting models. The value of 1 represents perfect
 421 agreement while -1 , perfect disagreement. A correlation of 0 means that the rankings are not related,
 422 which would be the expected score of the random ranking method.

423 The percentage of exact matches between ideal best performer and recommended best performer over
 424 all problems is defined as Success Rate. This is to evaluate the “precision” of the meta-learning
 425 performance. As a matter of fact, in the case of forecasting, users are sometimes more concerned if the
 426 recommended best performer (top 1) matches the ideal one, so only one model is built and computational
 427 efficiency is ensured. Therefore, besides the Spearman’s rank correlation coefficient, the success rate is
 428 also proposed to comprehensively evaluate the performance of the meta-learning system.
 429

430 3 EXPERIMENTS AND RESULTS

431 In this study, we investigate the cooling electricity consumption of buildings in the summer time.
 432 Simulation data are obtained by simulating the reference building energy consumption models for one
 433 month in July. The data are generated at a half-hour granularity using DOE’s EnergyPlus[55] simulation
 434 software, which yields 48 data points on each day, 1,488 data points for a month. Three forecasting cases
 435 are tested respectively: (1) Single day and a one week test, (2) an extrapolation test, and (3) a real
 436 building validation test.
 437

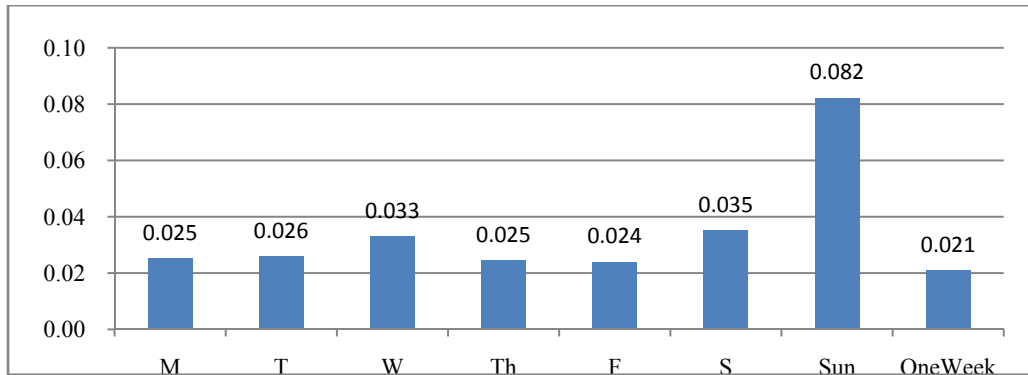
438 3.1 Experiment I

439 In this set of experiments, we test the performance of the proposed BEMR to forecast the building
 440 cooling load for each day of the last week and the whole last week of July, respectively. The single day
 441 test and one week test correspond to short-term load forecasting on a daily basis and a weekly basis. In
 442 the one week test, since the training data is scarce compared to the size of test case, we apply a traditional
 443 validation technique, where the first 80% of the data is used for training and the last 20% of the data is
 444 used for validation.

445 Figure 4 displays a bar chart of the mean of the NRMSE measures of the best forecasting model across
 446 the 48 problems on each test case. Except for the test on Sunday, the means of the best NRMSE are evenly
 447 distributed from 0.020 to 0.035, while the best performance on Sunday is significantly worse than those

448 on other days. To explain this observation, we may refer to the time series plot of the energy consumption
 449 in July. See Figure 5(a) for the weekly energy time series plot of the large office building in San Francisco,
 450 CA, which shows that the cooling load of Sunday is significantly less than other weekdays. The sudden
 451 decline may be due to the fact that most people don't come to work on weekends thus less cooling load is
 452 required. On the other hand, due to its significantly different pattern from the weekdays, data available for
 453 forecasting the energy consumptions for Sunday is scarce. This implies more training data with similar
 454 patterns are needed for energy forecasting on weekends. Figure 5(b) shows the time series plot of the
 455 cooling load of the same type of building located in Phoenix, AZ. Compared to plot (a), similar daily and
 456 weekly quasi-periodic behaviors are observed on the energy consumptions, with approximately constant
 457 variance and repeated patterns. However, the cooling load of the large office in Phoenix is on average one-
 458 tenth more than that in San Francisco, which is to be expected due to the hot summer in Phoenix. Figure
 459 5(c), which displays the cooling load time series plot of a full service restaurant in Phoenix, AZ, shows a
 460 markedly different behavior. The daily cooling load presents a stable pattern while the weekly periodicity
 461 is not as significant. This is likely due to the fact that restaurants are usually open seven days a
 462 week. Moreover, it is observed that the magnitude of the energy consumption in a restaurant is significant
 463 lower than that in a large office. These validate our proposition that cooling energy consumption is
 464 impacted by combined social factors, weather conditions and building types.

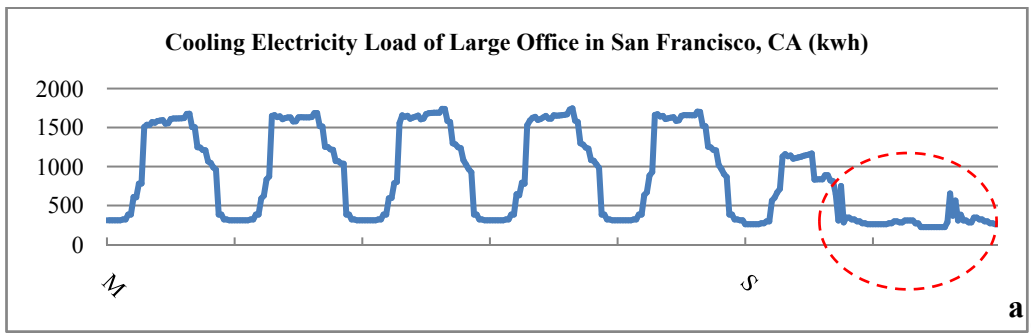
465



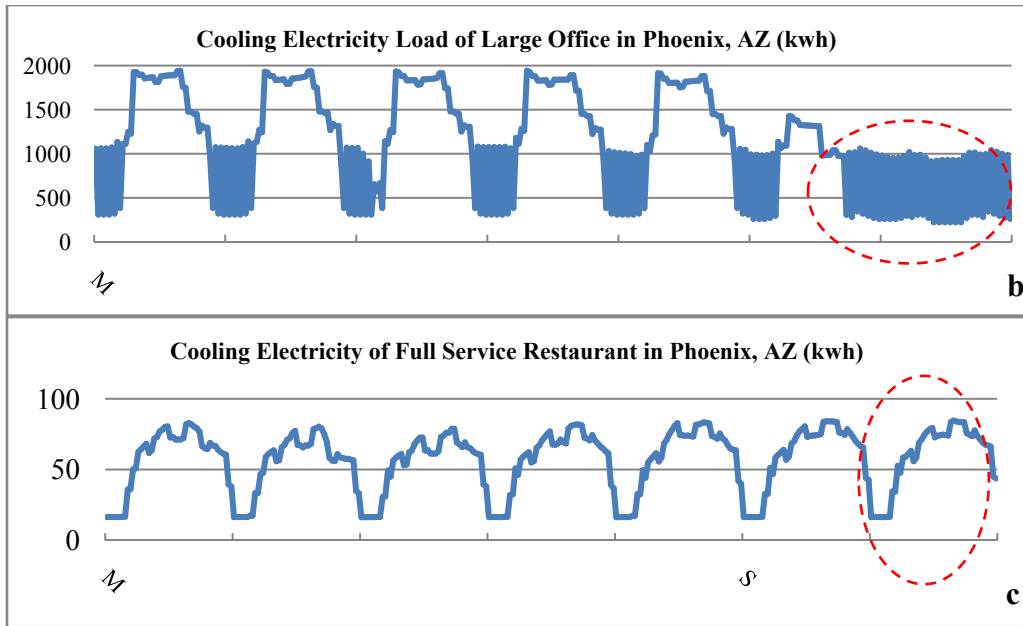
466

467 Figure 4 Test Case I: Bar Chart of Mean of Best NRMSE across 48 Problems on Each Test Case

468



469



470

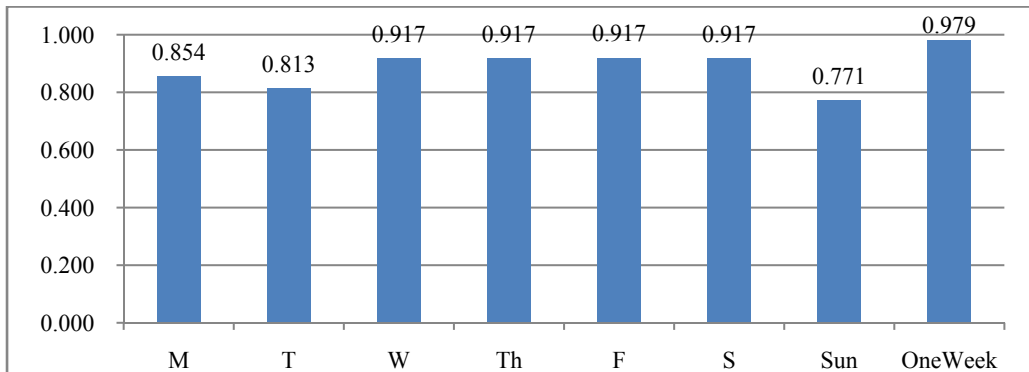
471

472 Figure 5 Weekly Cooling Electricity Load (Kwh) Time Series Plot of (a) Large Office in San Francisco,
 473 CA; (b) Large Office in Phoenix, AZ; (c) Full Service Restaurant in Phoenix, AZ.

474

475 Figure 6 and Figure 7 present the meta-learning performance in terms of success rate and SRCC.
 476 Table 3 summarizes the statistics of the above two performance measures. The average success rate
 477 amounts to 90%, which means almost 43 out of 48 problems are correctly assigned with the best model.
 478 Again, Sunday has the lowest success rate due to its different patterns from other days. In another words,
 479 its meta-features are less similar to others' causing difficulty in meta-learning. It is also observed that all the
 480 performance measures on the one week test are slightly better than those on the single day, however,
 481 notice that the training cost for the one week forecast is much higher than the single day forecast due to
 482 the higher training size. Be advised that there are always trade-offs between the computational cost and
 483 model performance, which is worth consideration when selecting the training and testing sizes. Please refer
 484 to Racine (2000) for a discussion on training, validation and testing sample size selection for time series
 485 forecasting using "hv-block" cross validation. In addition, the mean SRCC is around 96%, which implies
 486 high agreement between the predicted rankings of the recommendation system and the true rankings of
 487 the six forecasting models.

488



489

490 Figure 6 Test Case I: Bar Chart of Meta-learning Success Rate

491

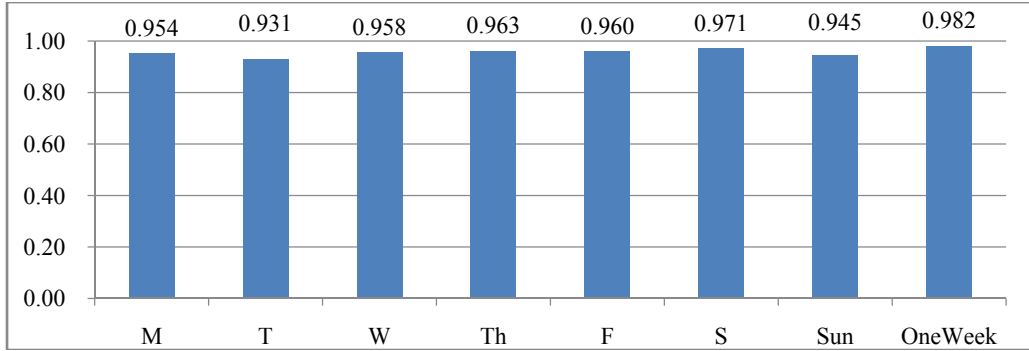


Figure 7 Test Case I: Bar Chart of Meta-learning SRCC

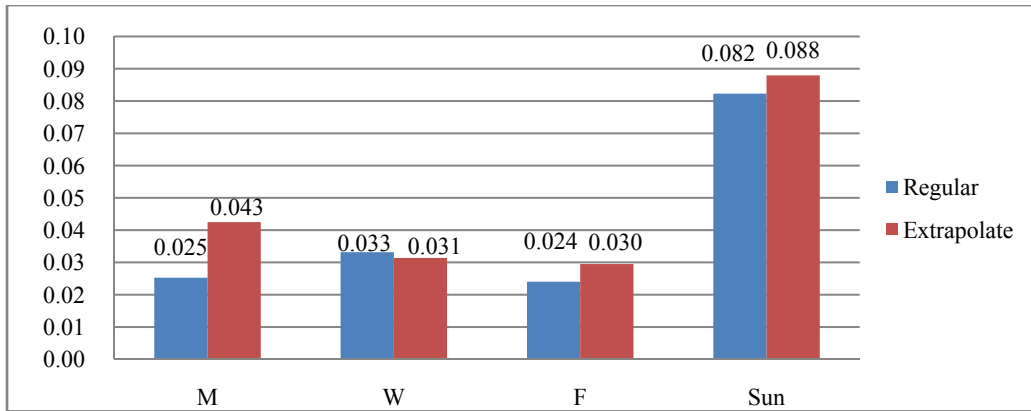
Table 3 Test Case I: Statistics on Meta-learning SRCC, Success Rate and # of Successes across 48 Problems

Test Date	M	T	W	Th	F	S	Sun	OneWeek	Mean
Spearman Correlation Coefficient	0.954	0.931	0.958	0.963	0.960	0.971	0.945	0.982	0.958
Success Rate	0.854	0.813	0.917	0.917	0.917	0.917	0.771	0.979	0.900
# of Successes (out of 48)	41	39	44	44	44	44	37	47	43

3.2 Experiment II

In this set of experiments, we test the extrapolation capability of the proposed BEMR. We sampled four days: Monday, Wednesday, Friday and Sunday of the last week, to forecast the building cooling load, while the training data is the building cooling load of the first week. Notice that by observing the energy data, some of the features of the last week are out of the range covered by the training data of the first week. For example, the average range of the difference between the maximum and minimum outdoor temperature among all the buildings in the first week is around [24, 35] °C, while it is around [22, 39] °C in the last week. The temperature gap in the training data allows us to test the extrapolation capability of the forecasting models and the recommendation system performance under uncertainties.

Figure 8 displays a bar chart of the mean of the NRMSE measures of the best forecasting model across 48 problems on the second test case. An attractive finding is that the best forecasting performance on extrapolation is only slightly inferior to regular forecasting. This can be observed by noting that the difference between the mean values in Figure 4 and Figure 8 is around 0.01. This indicates the best forecasting model generally is able to give a reliable forecast even though a time gap exists between the forecast horizon and the energy data at hand. Therefore, energy users and utilities can have confidence in the extrapolation predictions to pre-plan and make decisions in advance, which enables energy savings and cost reductions. Figure 9 displays a box plot of the mean of the NRMSE on the single day, one week and extrapolation tests across six forecasting algorithms. It is observed that the variance of the mean NRMSE for the tests on one day tests of Friday, Saturday, Sunday and the Sunday extrapolation are greater than other days, which indicates that the performance of different forecasting models vary significantly to each other on these days. This may be caused by the dates being weekends, or quasi-weekend (Friday), when the energy usage patterns are different from regular weekdays.

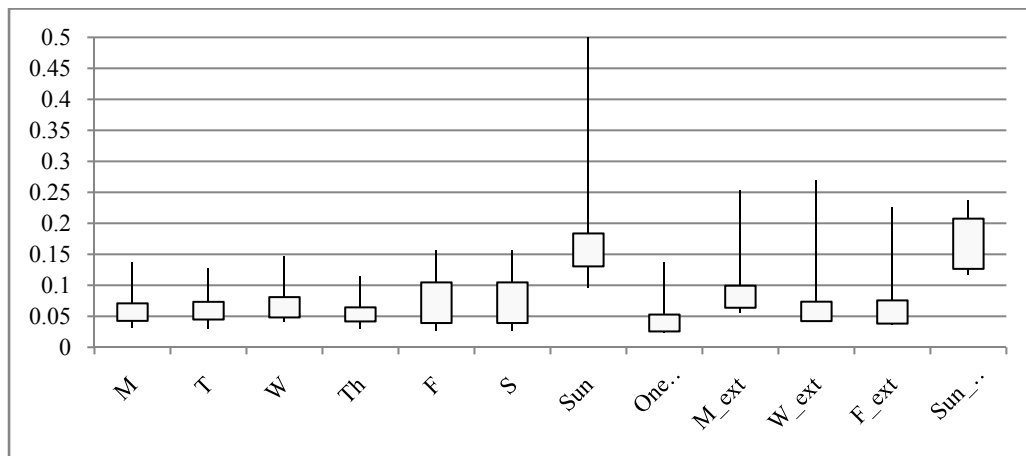


523

524

Figure 8 Test case II: Bar Chart of Mean of Best NRMSE across 48 Problems on Each Test Case

525



526

527

Figure 9 Box Plot of Mean of NRMSE on Test Cases I&II

528

529

530

531

532

533

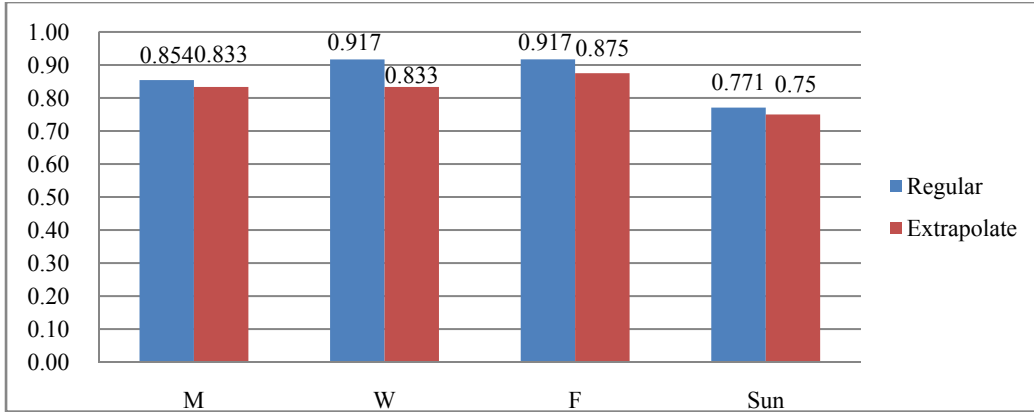
534

535

536

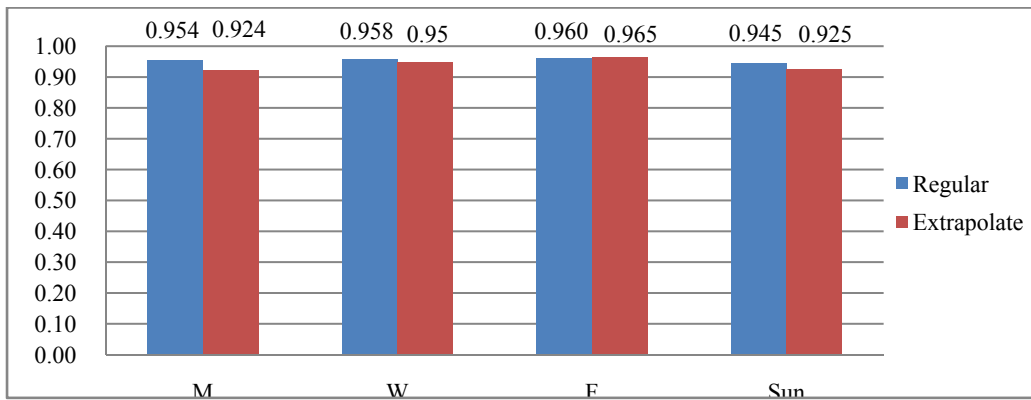
537

Figure 10 and Figure 11 present the meta-learning performance in terms of success rate and SRCC on the second test case. Table 4 summarizes the statistics of the above two performance measures. Similar to the comparison result on the best forecasting model performance, all three performance measures are slightly inferior to regular forecasting. The mean SRCC still remains above 94%, and the average successful recommendations are almost 40 out of 48, which is acceptable. Table 5 gives a comparison between the ground truth and the recommendation system of the three test cases based on the mean of the best NRMSE across 48 problems. It is shown that the average discrepancy between the recommended model and the true best model performance is within an error of 0.02, which reveals the proposed system is highly capable of making correct recommendations.



538
539
540

Figure 10 Test case II: Bar Chart of Meta-learning Success Rate



541
542
543

Figure 11 Test case II: Bar Chart of Meta-learning SRCC

544
545

Table 4 Test case II: Statistics on Meta-learning SRCC, Success Rate and # of Successes across 48 Problems

Test Date	M_ext	W_ext	F_ext	Sun_ext	Mean
Spearman Correlation Coefficient	0.924	0.950	0.965	0.925	0.941
Success Rate	0.833	0.833	0.875	0.750	0.833
# of Successes(out of 48)	40	40	42	36	40

546

547
548

Table 5 Comparison between Ground Truth and Recommendation System on Mean of Best NRMSE across 48 Problemson Each Test Case

Test Date	M	T	W	Th	F	S
True Best	0.025	0.026	0.033	0.025	0.024	0.035
Recommend	0.026	0.029	0.034	0.026	0.025	0.036
Test Date	Sun	OneWeek	M_ext	W_ext	F_ext	Sun_ext
True Best	0.082	0.021	0.043	0.031	0.030	0.088

Recommend	0.092	0.021	0.045	0.035	0.031	0.092
------------------	-------	-------	-------	-------	-------	-------

549
550 Table 6 summarizes the mean and standard deviation of the computational cost (in seconds) of the six
551 models on an Intel i5 CPU 16G computer. As seen, PR is the most computationally efficient model,
552 followed by RBF and Kriging. The least efficient algorithm is SVR, which takes more than 5 minutes on
553 average to solve each problem. The variance of the computational costs among different models implies
554 that a trial-and-error method is not an efficient approach for solving heterogeneous energy forecasting
555 problems, especially when the number of problems at hand is large and the problems have different levels
556 of complexity and heterogeneities. By summing the solution times of all six models, it is easy to see why a
557 trial-and-error approach for these types of problems is costly. By introducing the automatic model
558 recommendation using a meta-learning approach, the computational cost for forecasting reduces from an
559 order of minutes to seconds.
560

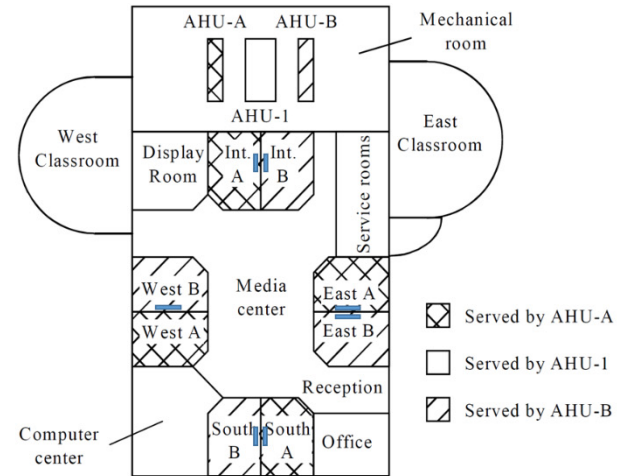
561 Table 6 Mean and Standard Deviation of the Computational Cost (in seconds) of the Six Models across 48
562 Problems

Statistics	Kriging	SVR	RBF	MARS	ANN	PR
Mean	2.75	324.94	0.68	202.79	10.44	0.28
Std.	0.27	151.29	0.08	119.22	1.50	0.08

563
564 The promising performance indicates that the proposed ANN based meta-learning recommendation
565 system is capable of accurately recommending not only the best model but also the ranking of the
566 models. This provides more freedom for users to select either one or several models, such as building an
567 ensemble of multiple models [56]. Moreover, it can be concluded that the meta-learning approach can
568 achieve both high prediction accuracy and high computational efficiency on heterogeneous forecasting
569 problems.
570

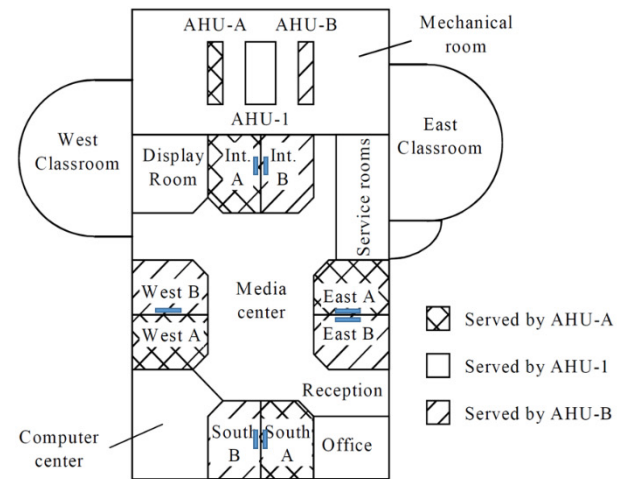
571 3.3 Experiment III

572 In this experiment, we test and validate the proposed BEMR using a real commercial building at the
573 Iowa Energy Center. The building operation data is acquired from ASHRAE 1312 [57]. The target is a
574 small size commercial building with an experiment area and common office area. The total floor space of
575 this building is 855.5 m². The area of each test room is 24.7 m². The percentage of exterior window area
576 to exterior wall area is 54 % for each exterior zone. A built-up roof with insulation is constructed above
577 the roof deck. The zone thermometers are located on the center of the internal wall (shown as the blue box
578 on the floor plan in
579



580
581
582
583
584
585
586
587
588
589
590
591
592

Figure 12). The location of the sensor is 1.21 meters from the floor. Two Variable Air Volume (VAV) air handling units (AHU) are used for the two experiment systems (A and B) in the experiment area. Both of these AHUs are equipped with dual (supply and return) variable speed fans and are operated similarly to that in a typical commercial building. More details about this building can be found at [58]. In the ASHRAE 1312 experiment, both AHU-A and AHU-B were used. However, AHU-A was used for faulty test and AHU-B was used for regular operation test. As a result, the summer (August and September) test data from AHU-B (system B) was used in this study. Similar to the subsystem operation schemes in experiment I and II, the chilled water temperature set point was 7.2 °C, the supply air temperature set point was 12.7 °C, the supply air pressure set point was 9.6 kPa, and the zone temperature heating and cooling set points at occupied hours (8 am to 6 pm) were 22.2 °C and 21.2 °C, respectively. The HVAC system was shut down during unoccupied hours.



593
594
595
596
597
598
599
600
601

Figure 12 Energy resource station at Iowa Energy Center [58]

We follow the exact same experimental settings, including the collection of operational features, the derivation of the meta-features, the training data selection and cross-validation. Again, the validation is conducted on both a single day test and one week test. Since the measurement data is collected between August and September, while the BEMR is built based on July, this could be viewed as an extrapolation test. The performance rankings of the six forecasting model along with the predicted rankings from BEMR are provided in Table 7.

602 Table 7 Performance Rankings (T) of the Six Forecasting Models and the Predicted Rankings from BEMR
 603 (B) on Single Day and One Week Tests

Model	Mon		Tue		Wed		Thu		Fri		Sat		Sun		One Week	
	T	B	T	B	T	B	T	B	T	B	T	B	T	B	T	B
Kriging	1	1	2	2	2	2	2	1	1	1	3	2	3	4	1	1
SVR	5	5	5	5	6	5	5	4	3	4	2	3	1	2	6	6
RBF	4	3	4	3	5	6	4	5	5	6	6	6	6	5	5	5
MARS	2	6	6	6	4	4	3	3	6	5	1	1	3	3	1	2
ANN	6	4	3	4	1	1	6	6	2	2	5	5	2	1	4	3
PR	2	2	1	1	3	3	1	2	3	3	3	4	5	6	3	4

604 The statistics show that 2 out of 8 test cases (Thursday and Sunday) are assigned a sub-optimal model,
 605 while the assigned models are both ranked second according to the ground truth, which implies the
 606 BEMR generally provides reliable recommendations. In conclusion, the validation experiment results on
 607 the real building indicate that the proposed BEMR is able to assist real building energy forecasting tasks
 608 with reliable and high quality solutions.
 609
 610

611 4 DISCUSSION, CONCLUSION AND FUTURE WORK

612 This paper is motivated to develop a computationally efficient data-driven approach to quickly
 613 identify appropriate algorithms for building energy load forecasting. We propose a recommendation
 614 system for short-term building forecasting model selection based on a meta-learning technique. This is an
 615 extensively studied automatic learning algorithm applied to meta-data in machine learning experiments.
 616 We propose various meta-features which characterize the building energy data: building electricity load
 617 time series features, building operational features and physical features. An Artificial Neural Network is
 618 applied to model the relationship between the meta-features and the ranking of each model derived from
 619 the performance on forecasting. In addition, due to the high dimensionality of the proposed meta-features,
 620 an advanced feature reduction technique, Singular Value Decomposition, is applied on the meta-feature
 621 space to improve the meta-learning performance and reduce computational cost. The resulting high
 622 spearman’s ranking correlation coefficient and success rate on the two test cases: single day and one week,
 623 and the extrapolation test, indicate the successful implementation of the recommendation system.

624 To demonstrate the applicability of the proposed recommendation system, 48 benchmark
 625 buildings have been tested, including 8 types of typical buildings located across 6 climate zones covering a
 626 wide range of building profiles. One real building is used to validate the system for assessment of the
 627 applicability and extensibility to real problems. To evaluate the forecasting capability of the proposed
 628 framework, we have also implemented various popular data-driven forecasting methods in the literature,
 629 including Kriging, SVR, RBF, MARS, ANN and PR. Regarding the practical advantages of this
 630 framework and its combination with energy supplies in the domain of building energy and power
 631 systems, the proposed recommendation system can be used to facilitate the development of a building
 632 energy expert system for real-time building operations management, decision making and
 633 support. Comparing this technique to the traditional approach, it is concluded that the meta-learning
 634 approach can achieve both high prediction accuracy and high computational efficiency on various genres
 635 of building forecasting problems. It augments the traditional trial-and-error meta-modeling method in that
 636 it enables an automated and optimized modeling process which requires little expert involvement and
 637 minimizes excessive computations. Based on past experience, the recommendation system emulates the
 638 human’s decision-making ability, which makes reasonable decisions and efficient calculations to solve
 639 complex problems. Specifically, it consists of a two stage learning process: the knowledge base is first
 640 constructed, which accumulates facts and rules about the problem domain, and then an inference engine is
 641 built to apply the rules from the known facts and deduce new facts. This work provides practical guidelines

642 in the design, development, implementation, and testing of a forecasting recommendation system for
643 various short-term building energy forecasting problems. Specifically, it can help non-experts with
644 forecasting model selection. Due to these theoretical contributions and advantages, we recommend its use
645 to facilitate everyday building energy industrial applications and operations to reduce the cost and improve
646 modeling and operation efficiency.

647 In summary, the originality of this paper is three-fold:

- 648 • The first contribution is the implementation of a two-stage meta-learning framework on various time-
649 series problems in the domain of building energy modeling.
- 650 • The second contribution stems from the proposed generalized automatic meta-learning based expert
651 system which requires little human involvement to support forecasting model recommendation.
- 652 • To the best of our knowledge, this is the first recommendation system motivated from the machine
653 learning domain for short-term building forecasting based on various meta-features derived from both
654 of building data-characteristics and physical-characteristic features.

655 We acknowledge that conducting our analysis in the scope of STLTF is a limitation of this study.
656 However, the proposed approach adequately demonstrates the applicability of the recommendation system
657 on energy forecasting for various types of buildings across different climate zones. We envision that the
658 STLTF framework is viably transformable to MTLTF and LTLTF by adjusting the operational features and
659 meta-features, and we reserve this for our future work.
660

661 APPENDIX DATA-DRIVEN MODELING TECHNIQUES

662 The data-driven modeling techniques build models solely on historical data which is represented by
663 the time-delay variables, e.g., temperature, humidity, and past energy consumption data, that form the
664 feature vectors. This makes the forecasting process more adaptive to different types of buildings and
665 reduces human involvement for model adjustments [6]. Six selected data-driven modeling techniques,
666 including four of statistical modeling methods, Kriging, RBF, MARS and PR, and two machine learning
667 methods, SVR and ANN, are reviewed in this section. Notice in each method that we are building a model
668 of the building energy consumption based on the building's operational features.

669 Kriging

670 Kriging (also known as Gaussian process regression) is an interpolation method that assumes the
671 simulation output may be modeled by a Gaussian process. It gives the best linear unbiased prediction of
672 simulation output not yet observed. It generates the prediction in the form of a combination of a global
673 model with local random noise:

$$674 \quad \mathbf{y}(x) = \mathbf{f}(x)\boldsymbol{\beta} + \mathbf{Z}(x), \quad (1)$$

675 where x is the input vector, $\boldsymbol{\beta}$ is the weight vector, and $\mathbf{Z}(x)$ is a stochastic process with zero mean and
676 stationary covariance of

$$677 \quad \text{cov}[\mathbf{Z}(x_i), \mathbf{Z}(x_j)] = \sigma^2 \mathbf{R}(x_i, x_j), \quad (2)$$

678 where σ^2 is the process variance, $\mathbf{R}(x_i, x_j)$ is an n by n correlation matrix where n is the sample size of
679 the training data. \mathbf{R} is usually depicted by a Gaussian correlation function, $\exp(-\theta(x_i - x_j)^2)$ with
680 parameter θ .

681 Support Vector Regression

682 Support Vector Regression (SVR) is analogous to support vector classification, which attempts to
683 maximize the distance between two classes of data by selecting two hyperplanes to optimally separate the
684 training data. The mathematical form of SVR is:
685

686
$$f(x) = \langle \omega \cdot x \rangle + b, \quad (3)$$

687 where ω is the norm vector to the hyperplane and $b/\|\omega\|$ determines the offset of the hyperplane from the
 688 origin. The goal is to find a hyperplane that separates the data points optimally without error and separates
 689 the closest points with the hyperplane as far as possible. Thus, it can be constructed as an optimization
 690 problem:

691
$$\min 1/2|\omega|^2$$

 692 s.t.
$$\begin{cases} y_i - \langle \omega \cdot x_i \rangle - b \leq \varepsilon \\ \langle \omega \cdot x_i \rangle + b - y_i \leq \varepsilon \end{cases} \quad (4)$$

693 According to the duality principle, the nonlinear regression problem is given by:

694
$$f(x) = \sum_{i=1}^m (\alpha_i^* - \alpha_i) k(x_i \cdot x_j) + b. \quad (5)$$

695 where α_i^* and α_i are two introduced dual variables, and $k(x_i \cdot x_j)$ is a kernel function, e.g. Gaussian
 696 kernel.

697 **Radial Basis Function**

698 Radial Basis Function (RBF) is used to develop interpolation on scattered multivariate data. A RBF is a
 699 linear combination of a real-valued radially symmetric function, $\phi(x)$, based on distance from the origin,

700
$$f(x) = \sum_{i=1}^n \theta_i \phi(\|x - x_i\|). \quad (6)$$

701 where θ_i is the unknown interpolation coefficient determined by the least-squares method, n is the
 702 number of sampling points and $\|x - x_i\|$ is the Euclidean norm of the radial distance from design point x
 703 to the sampling point x_i .

704 **Multivariate Adaptive Regression Splines**

705 Multivariate Adaptive Regression Splines (MARS) is a form of regression analysis introduced by
 706 Friedman(1991). A set of basis functions, defined as constant, hinge function, or the product of two or
 707 more hinge functions, are combined in the weighted sum form, to be the approximation of the response
 708 function. A MARS model is built with generalized cross validation regularization in a forward/backward
 709 iterative process. The general model of MARS can be written as:

710
$$f(x) = \gamma_0 + \sum_{i=1}^m \gamma_i h_i(x), \quad (7)$$

711 where γ_i is the constant coefficient of the combination whose value is jointly adjusted to give the best
 712 fit to the data, and the basis function h_i , can be represented as:

713
$$h_i(x) = \prod_{k=1}^{K_m} [s_{k,m} (x_{v(k,m)} - t_{k,m})]_+^q. \quad (8)$$

714 where K_m is the number of splits given to the m^{th} basis function, $s_{k,m} = \pm 1$ indicates the right/left sense of
 715 the associated step function, $v(k,m)$ is the label of the variable, and $t_{k,m}$ represents values (knot
 716 locations) of the corresponding variables. The superscript q and subscript $+$ indicate the truncated power
 717 functions with polynomials of lower order than q .

718 **Artificial Neural Network**

719 Artificial Neural Network (ANN) [60] is a computational model inspired by an animal's central
 720 nervous system. It is apt at solving problems with complicated structures. Due to its promising results in
 721 numerous fields, ANN has been extensively applied in stochastic simulation modeling (Fonseca,
 722 Navarrese, & Moynihan, 2003; Nasereddin & Mollaghasemi, 1999). An ANN model typically consists of
 723 three separate layers: the input layer, the hidden layer(s), and the output layer. The neurons across

724 different layers are interconnected to transmit and deduce information. A typical ANN with three layers
725 and one single output neuron has the following mathematical form:

$$726 \quad f(x) = \sum_{j=1}^J \omega_j \delta(\sum_{i=1}^I w_{ij} \delta(x_i) + \alpha_j) + \beta + \varepsilon. \quad (9)$$

727 where x is a k -dimensional vector, the input unit represents the raw information that is fed into the
728 network, $\delta(\cdot)$ is the user defined transfer function, w_{ij} is the weight factor on the connection between the
729 i^{th} input neuron and the j^{th} hidden neuron, α_j is the bias in the j^{th} hidden neuron, ω_j is the weight on
730 connection between the j^{th} hidden neuron and the output neuron, β is the bias of the output neuron, ε is a
731 random error with a mean of 0, and I and J are the number of input neurons and hidden neurons. In
732 supervised learning, the output unit is trained to simulate the underlying structure of the input signals and
733 response. The trained structure is depicted by several parameters, the weights on each connection, the
734 biases, the number of hidden layers, the transfer functions, and the number of hidden nodes in each
735 hidden layer.

736 Polynomial Regression

737 Polynomial Regression (PR) is a variation of linear regression in which an n^{th} order polynomial is
738 modeled to formulate the relationship between the independent variable x and the dependent variable y .
739 PR models have been applied to various engineering domains such as mechanical, medical and industrial
740 (Barker et al., 2001; Greenland, 1995; Shaw et al., 2006). A second-order polynomial model can be
741 expressed as:

$$742 \quad f(x) = \beta_0 + \sum_{i=1}^k \beta_i x_i + \sum_{i=1}^k \beta_{ii} x_i^2 + \sum_i \sum_j \beta_{ij} x_i x_j + \epsilon \quad (10)$$

743 where β is the constant coefficient, k is the number of variables, ϵ is an unobserved random error with
744 zero mean, PR models are usually fit using the least squares method.
745 Extensive applications on forecasting using the reviewed techniques can be found in [5], [18], [65], [66].
746

747 Acknowledgement

748 This research was partially supported by funds from the National Science Foundation award under grant
749 number CNS-1239257 and from the United States Transportation Command (USTRANSCOM) in concert
750 with the Air Force Institute of Technology (AFIT) under an ongoing Memorandum of Agreement. The
751 U.S. Government is authorized to reproduce and distribute for governmental purposes notwithstanding
752 any copyright annotation of the work by the author(s). The views and conclusions contained herein are
753 those of the authors and should not be interpreted as necessarily representing the official policies or
754 endorsements, either expressed or implied, of USTRANSCOM, AFIT, the Department of Defense, or the
755 U.S. Government.
756

757 References

- 758 [1] Architecture 2030, “2030 Challenge for Products: Critical Points,” 2011.
- 759 [2] X. Li, J. Wen, and E.-W. Bai, “Developing a whole building cooling energy forecasting model for on-
760 line operation optimization using proactive system identification,” *Appl. Energy*, vol. 164, no.
761 2016, pp. 69–88, 2016.
- 762 [3] X. Li and J. Wen, “Review of building energy modeling for control and operation,” *Renew. Sustain.*
763 *Energy Rev.*, vol. 37, pp. 517–537, 2014.
- 764 [4] B. Eisenhower, Z. O’Neill, S. Narayanan, V. a. Fonoberov, and I. Mezić, “A methodology for meta-
765 model based optimization in building energy models,” *Energy Build.*, vol. 47, pp. 292–301, Apr.
766 2012.

- 767 [5] L. Yu, S. Wang, and K. K. Lai, "A neural-network-based nonlinear metamodeling approach to
768 financial time series forecasting," *Appl. Soft Comput.*, vol. 9, no. 2, pp. 563–574, Mar. 2009.
- 769 [6] D. Solomon, R. Winter, A. Boulanger, R. Anderson, and L. Wu, "Forecasting Energy Demand in
770 Large Commercial Buildings Using Support Vector Machine Regression," 2000.
- 771 [7] J. Crespo Cuaresma, J. Hlouskova, S. Kossmeier, and M. Obersteiner, "Forecasting electricity spot-
772 prices using linear univariate time-series models," *Appl. Energy*, vol. 77, no. 1, pp. 87–106, Jan.
773 2004.
- 774 [8] W.-C. Hong, "Electric load forecasting by seasonal recurrent SVR (support vector regression) with
775 chaotic artificial bee colony algorithm," *Energy*, vol. 36, no. 9, pp. 5568–5578, Sep. 2011.
- 776 [9] T. Salsbury and R. Diamond, "Performance Validation and Energy Analysis of HVAC Systems using
777 Simulation 1 Introduction 2 Simulation-Based Validation Methodology," *Indoor Environ.*, vol. 25,
778 pp. 1–20, 1996.
- 779 [10] M. Hu, "A data-driven feed-forward decision framework for building clusters operation under
780 uncertainty," *Appl. Energy*, vol. 141, no. 2015, pp. 229–237, 2015.
- 781 [11] M. Hu and H. Cho, "A probability constrained multi-objective optimization model for CCHP
782 system operation decision support," *Appl. Energy*, vol. 116, pp. 230–242, 2014.
- 783 [12] T. Hong, "Short Term Electric Load Forecasting," 2010.
- 784 [13] H. Lee Willis, *Power Distribution Planning Reference Book*. CRC press, 2004.
- 785 [14] H. Wang, P. Xu, X. Lu, and D. Yuan, "Methodology of comprehensive building energy
786 performance diagnosis for large commercial buildings at multiple levels," *Appl. Energy*, vol. 169,
787 no. 2016, pp. 14–27, 2016.
- 788 [15] M. T. Hagan and S. M. Behr, "The Time Series Approach to Short Term Load Forecasting," vol.
789 PWR5-2, no. 3, pp. 785–791, 1987.
- 790 [16] R. J. Hyndman, A. B. Koehler, R. D. Snyder, and S. Grose, "A state space framework for
791 automatic forecasting using exponential smoothing methods," *Int. J. Forecast.*, vol. 18, no. 3, pp.
792 439–454, 2002.
- 793 [17] S. Baldi, S. Yuan, P. Endel, and O. Holub, "Dual estimation: Constructing building energy models
794 from data sampled at low rate," *Appl. Energy*, vol. 169, pp. 81–92, 2016.
- 795 [18] L. E. Mavromatidis, A. Bykalyuk, and H. Lequay, "Development of polynomial regression models
796 for composite dynamic envelopes' thermal performance forecasting," *Appl. Energy*, vol. 104, pp.
797 379–391, 2013.
- 798 [19] H. S. Hippert, C. E. Pedreira, and R. C. Souza, "Neural networks for short-term load forecasting: a
799 review and evaluation," *IEEE Trans. Power Syst.*, vol. 16, no. 1, pp. 44–55, 2001.
- 800 [20] C. R. Touretzky and R. Patil, "Building-level power demand forecasting framework using building
801 specific inputs: Development and applications," *Appl. Energy*, vol. 147, pp. 466–477, 2015.
- 802 [21] A. D. Papalexopoulos and T. C. Hesterberg, "A regression-based approach to short-term system
803 load forecasting," *IEEE Trans. Power Syst.*, vol. 5, pp. 1535–1547, 1990.
- 804 [22] J. W. Taylor and P. E. McSharry, "Short-term load forecasting methods: An evaluation based on
805 European data," *IEEE Trans. Power Syst.*, vol. 22, pp. 2213–2219, 2007.
- 806 [23] N. K. Ahmed, A. F. Atiya, N. El Gayar, and H. El-Shishiny, "An Empirical Comparison of
807 Machine Learning Models for Time Series Forecasting," *Econom. Rev.*, vol. 29, no. 5–6, pp. 594–

- 808 621, Aug. 2010.
- 809 [24] S. Chirattananon and J. Taveekun, "An OTTV-based energy estimation model for commercial
810 buildings in Thailand," *Energy Build.*, vol. 36, no. 7, pp. 680–689, 2004.
- 811 [25] F. W. H. Yik, J. Burnett, and I. Prescott, "Predicting air-conditioning energy consumption of a
812 group of buildings using different heat rejection methods," *Energy Build.*, vol. 33, no. 2, pp. 151–
813 166, 2001.
- 814 [26] L. Tang, L. Yu, and K. He, "A novel data-characteristic-driven modeling methodology for nuclear
815 energy consumption forecasting," *Appl. Energy*, vol. 128, no. 2014, pp. 1–14, 2014.
- 816 [27] J. S. Armstrong, "Forecasting by Extrapolation: Conclusions from Twenty-five Years of
817 Research," vol. 14, no. 6, 1984.
- 818 [28] X. Lü, T. Lu, C. J. Kibert, and M. Viljanen, "Modeling and forecasting energy consumption for
819 heterogeneous buildings using a physical–statistical approach," *Appl. Energy*, vol. 144, no. 2015,
820 pp. 261–275, 2015.
- 821 [29] M. Matijaš, "Electric Load Forecasting using Multivariate Meta-learning," 2013.
- 822 [30] B. F. De Souza, A. De Carvalho, and C. Soares, "Metalearning for Gene Expression Data
823 Classification," *2008 Eighth Int. Conf. Hybrid Intell. Syst.*, pp. 441–446, Sep. 2008.
- 824 [31] Z. Lan, J. Gu, Z. Zheng, R. Thakur, and S. Coghlan, "A study of dynamic meta-learning for failure
825 prediction in large-scale systems," *J. Parallel Distrib. Comput.*, vol. 70, no. 6, pp. 630–643, Jun.
826 2010.
- 827 [32] S. Zhou, K. K. Lai, and J. Yen, "A dynamic meta-learning rate-based model for gold market
828 forecasting," *Expert Syst. Appl.*, vol. 39, no. 6, pp. 6168–6173, May 2012.
- 829 [33] Marin Matijaš, "Electric Load Forecasting Using Support Vector.pdf," 2013.
- 830 [34] F. Collopy and J. S. Armstrong, "Rule-Based Forecasting: Development and Validation of an
831 Expert Systems Approach to Combining Time Series Extrapolations," *Management Science*, vol.
832 38, no. 10, pp. 1394–1414, 1992.
- 833 [35] R. B. C. Prudêncio and T. B. Ludermir, "Meta-learning approaches to selecting time series
834 models," *Neurocomputing*, vol. 61, pp. 121–137, Oct. 2004.
- 835 [36] X. Wang, K. Smith-Miles, and R. Hyndman, "Rule induction for forecasting method selection:
836 Meta-learning the characteristics of univariate time series," *Neurocomputing*, vol. 72, pp. 2581–
837 2594, 2009.
- 838 [37] C. Lemke and B. Gabrys, "Meta-learning for time series forecasting and forecast combination,"
839 *Neurocomputing*, vol. 73, no. 10–12, pp. 2006–2016, Jun. 2010.
- 840 [38] M. Matijaš, J. a. K. Suykens, and S. Krajcar, "Load forecasting using a multivariate meta-learning
841 system," *Expert Syst. Appl.*, vol. 40, no. 11, pp. 1–11, 2013.
- 842 [39] C. Cui, M. Hu, J. D. Weir, and T. Wu, "A Recommendation System for Meta-modeling: A Meta-
843 learning based Approach," *Expert Syst. Appl.*, 2015.
- 844 [40] G. G. Wang and S. Shan, "Review of Metamodeling Techniques in Support of Engineering Design
845 Optimization," *J. Mech. Des.*, vol. 129, no. 4, p. 370, 2007.
- 846 [41] Anna Ściężko, "Surrogat modeling techniques applied to energy systems," University of Iceland &
847 University of Akureyri, 2011.

- 848 [42] H. X. Zhao and F. Magoulès, “A review on the prediction of building energy consumption,”
849 *Renew. Sustain. Energy Rev.*, vol. 16, no. 6, pp. 3586–3592, 2012.
- 850 [43] M. Deru, K. Field, D. Studer, K. Benne, B. Griffith, P. Torcellini, B. Liu, M. Halverson, D.
851 Winiarski, and M. Rosenberg, “U.S. Department of Energy Commercial Reference Building
852 Models of the National Building Stock,” 2011.
- 853 [44] ASHRAE., “Energy Efficient Design of New Buildings Except Low-Rise Residential Buildings.
854 ANSI/ASHRAE/IESNA Standard 90.1 -2004.” American Society of Heating, Refrigeration, and
855 Air-Conditioning Engineers, Atlanta, GA, 2004.
- 856 [45] S. Wilcox and W. Marion, “Users manual for TMY3 data sets,” 2008.
- 857 [46] D. C. Montgomery, E. a Peck, and G. G. Vining, *Introduction to Linear Regression Analysis*. John
858 Wiley & Sons, 2012.
- 859 [47] X. Li, C. Sun, and D. Gong, “Application of support vector machine and similar day method for
860 load forecasting,” in *Advances in Natural Computation*, Springer, 2005, pp. 602–609.
- 861 [48] J. Racine, “Consistent cross-validators for dependent data: hv -block cross-
862 validation,” *J. Econom.*, vol. 99, pp. 39–61, 2000.
- 863 [49] D. Kugiumtzis, “Surrogate data test for nonlinearity including nonmonotonic transforms,” *Phys.*
864 *Rev. E - Stat. Physics, Plasmas, Fluids, Relat. Interdiscip. Top.*, vol. 62, no. 1, pp. 25–28, 2000.
- 865 [50] D. J. Fonseca, D. O. Navarrese, and G. P. Moynihan, “Simulation metamodeling through artificial
866 neural networks,” *Eng. Appl. Artif. Intell.*, vol. 16, pp. 177–183, 2003.
- 867 [51] L. Yu, S. Wang, and K. Keung, “Forecasting crude oil price with an EMD-based neural network
868 ensemble learning paradigm,” vol. 30, pp. 2623–2635, 2008.
- 869 [52] G. Hughes, “On the mean accuracy of statistical pattern recognizers,” *IEEE Trans. Inf. Theory*,
870 vol. 14, 1968.
- 871 [53] C. Eckart and G. Young, “The approximation of one matrix by another of lower rank,”
872 *Psychometrika*, vol. 1, pp. 211–218, 1936.
- 873 [54] H. R. Neave and P. L. Worthington, *Distribution-free tests*. London: Routledge, 1989.
- 874 [55] R. K. S. et al. Crawley, Drury B., Linda K. Lawrie, Frederick C. Winkelmann, Walter F. Buhl, Y.
875 Joe Huang, Curtis O. Pedersen, “EnergyPlus: creating a new-generation building energy
876 simulation program,” *Energy Build.*, vol. 33, no. 4, pp. 319–331, 2001.
- 877 [56] C. Cui, T. Wu, M. Hu, J. D. Weir, and X. Chu, “Accuracy vs. robustness: bi-criteria optimized
878 ensemble of metamodels,” *Proc. 2014 Winter Simul. Conf.*, pp. 616–627, 2014.
- 879 [57] J Wen and S. Li, “Tools for evaluating fault detection and diagnostic methods for air-handling
880 units,” ASHRAE, 2012.
- 881 [58] B. A. Price and T. F. Smith, “Development and validation of adaptive optimal operation
882 methodology for building HVAC systems,” 2003.
- 883 [59] J. H. Friedman, “Multivariate Adaptive Regression Splines,” *Ann. Stat.*, vol. 19, pp. 1–67, 1991.
- 884 [60] F. Rosenblatt, “The perceptron: a probabilistic model for information storage and organization in
885 the brain,” *Psychol. Rev.*, vol. 65, no. 6, pp. 386–408, 1958.
- 886 [61] M. Nasereddin and M. Mollaghasemi, “The development of a methodology for the use of neural
887 networks and simulation modeling in system design,” in *1999 Winter Simulation Conference*

- 888 (WSC'99) - Volume 1, 1999, pp. 537–542.
- 889 [62] S. Greenland, “Dose-response and trend analysis in epidemiology: alternatives to categorical
890 analysis,” *Epidemiology*, vol. 6, pp. 356–365, 1995.
- 891 [63] P. A. Barker, F. A. Street-Perrott, M. J. Leng, P. B. Greenwood, D. L. Swain, R. A. Perrott, R. J.
892 Telford, and K. J. Ficken, “A 14,000-year oxygen isotope record from diatom silica in two alpine
893 lakes on Mt. Kenya,” *Science*, vol. 292, pp. 2307–2310, 2001.
- 894 [64] P. Shaw, D. Greenstein, J. Lerch, L. Clasen, R. Lenroot, N. Gogtay, A. Evans, J. Rapoport, and J.
895 Giedd, “Intellectual ability and cortical development in children and adolescents,” *Nature*, vol.
896 440, pp. 676–679, 2006.
- 897 [65] S. K. Sahu, “A Bayesian Kriged-Kalman model for short-term forecasting of air pollution
898 levels,” *Appl. Stat.*, vol. 54, pp. 223–244, 2005.
- 899 [66] W. Shen, X. Guo, C. Wu, and D. Wu, “Forecasting stock indices using radial basis function neural
900 networks optimized by artificial fish swarm algorithm,” *Knowledge-Based Syst.*, vol. 24, no. 3, pp.
901 378–385, 2011.
- 902